Chaos, Solitons and Fractals 106 (2018) 80–85

Contents lists available at ScienceDirect

Chaos, Solitons and Fractals

Nonlinear Science, and Nonequilibrium and Complex Phenomena

journal homepage: www.elsevier.com/locate/chaos

Coherence resonance in stimulated neuronal network

Andrey V. Andreev[a], Vladimir V. Makarov[a], Anastasija E. Runnova[a], Alexander N. Pisarchik[a,b], Alexander E. Hramov[a,c,*]

[a] Yuri Gagarin State Technical University of Saratov, Politechnicheskaya, 77, Saratov 410054, Russia
[b] Center for Biomedical Technology, Technical University of Madrid, Campus Montegancedo, Pozuelo de Alarcon, Madrid 28223, Spain
[c] Saratov State University, Astrakhanskaya, 83, Saratov 410012, Russia

ARTICLE INFO

Article history:
Received 25 August 2017
Revised 9 November 2017
Accepted 12 November 2017

Keywords:
Neural oscillator
Map
Coherence
Synchronization
Complex network
Neuronal network

ABSTRACT

We consider a neuronal network model where an external stimulus excites some neurons, which in turn activate other neurons in the network via synapse. We find that the regularity in macroscopic spiking activity of the whole neuronal network maximizes at a certain level of intrinsic noise. A similar resonant behavior, referred to as coherence resonance, is also observed with respect to the stimulus strength, network size, and number of stimulated neurons. The coherence is quantitatively estimated with the signal-to-noise ratio calculated from the average power spectra of the macroscopic signal and with autocorrelation time. Overall synchronization in the neuronal network also exhibits a non-monotonic dependence on the network size.

1. Introduction

As all real systems, the neural systems are noisy. Among many different sources of noise, the ones worth mentioning are quasi-random release of neurotransmitters by synapses, random synaptic input from other neurons, and random switching of ion channels. Noise plays an advantageous role in the nervous system and is needed for its good functionality in all levels of organization, starting with cells and ending with the brain. Stochastic processes in the brain may have different origins, such as, probabilistic random spontaneous neural activity and random synaptic connections [1]. Inherent brain noise plays an important advantageous role in signal detection and decision-making by preventing deadlocks, underlying important mechanisms of brain functionality and self-organization [2–4].

In recent years, the effects of noise in neural systems have attracted a lot of attention of neurophysiologists and physicists, especially due to its benefits, such as coherence and stochastic resonances [5–8,10]. In *coherence resonance* the regularity of a noisy or a chaotic system maximizes at a certain value of a random or a chaotic force. When the force is random, it is referred to as *stochastic coherence resonance* [6,7,10], while in a chaotic system it is called *deterministic coherence resonance* [11–13]. Coherence resonance can occur either in a bistable or an excitable system close to the excitation threshold. Stochastic resonance [5,8,14,15] is a particular case of coherence resonance when a periodic signal is present. It is characterized by a maximum in the signal-to-noise ratio with respect to noise or chaos intensity. Stochastic resonance is always accompanied by coherence resonance.

In a notable paper [5], Simonotto et al. showed that noise improves perception when a visual stimulus is below the perception threshold. They interpreted this result as stochastic resonance in a nervous system. Although this work stimulated further research in this direction, including the present one, there are some uncertainties in this interpretation. First of all, the perception stimulus is not periodic. Therefore, in fact they deal with coherence resonance, but not with stochastic resonance. Second, the darkness of the image background (or fog) is not noise, it is rather associated with the perception threshold. So, you may ask: Where is the noise? Noise is in the brain. We may also suggest the brain adjusts intrinsic noise to increase signal-to-noise ratio while receiving a very weak stimulus. However, this is only half of the story.

In 2003, Toral et al. [10] found noise-induced coherence resonance in a network of FitzHung–Nagumo oscillators. They showed that the network coherence maximized at a certain network size. A similar size-dependent resonance effect was previously observed in an ensemble of coupled bistable noise-driven oscillators subjected to a periodic force [8]. The authors of the above papers suggested that not only noise, but also the network size can be adjusted to enhance the sensitivity of a neural system in signal recognition. It is not yet clear how the brain adjusts network size. We may

---

[*] Corresponding author.
E-mail address: hramovae@gmail.com (A.E. Hramov).

https://doi.org/10.1016/j.chaos.2017.11.017

suppose that synaptic plasticity plays a key role in this process, or the brain adjusts a number of excited neurons or a number of autapses. Autapse-induced coherence resonance was recently demonstrated in a scale-free network of stochastic Hodgkin–Huxley neurons [9].

In this paper, we focus in studying coherence phenomenon in a network of globally coupled neural oscillators with randomly distributed coupling strengths under the influence of intrinsic noise. In particular, we investigate how noise intensity, network size, and the number of stimulated neurons affect the network regularity (coherence). As a basic model we choose the Rulkov map [16]. We should note that map-based neuron models are highly effective for numerical simulations of neural dynamics and functionality in neurobiological networks because they allow studying the interaction between individual neurons and mean field oscillations formed in large-scale networks. They can also be used for implementation of biological neuronal mechanisms responsible for signal processing of sensory information, such as visual, auditory and tactile, as well as for designing real-time synthetic neurobiological controllers for biometric robots and neuronal prosthetic devices.

Recently, the neuronal bursting activity was studied in a network of globally coupled Rulkov maps [17]. The authors of the paper investigated the network synchronization by analyzing the macroscopic signal of the whole network. Such an approach is very convenient when microscopic access to individual neurons is not possible, e.g., to simulate experiments with neural cultures grown on a multielectrode matrix. The synchronized collective bursting activity of many neurons has been shown to be associated with some pathological states, e.g., epilepsy [18] and migraine [19]. In the present work, we use the same macroscopic approach to reveal the mechanisms responsible for the regularity of the collective bursting dynamics or the network coherence.

The coherence can be estimated using different approaches. The common measures for the coherence used in previous papers were the characteristic correlation time, normalized fluctuation of phase duration (or jitter) [6,10] and signal-to-noise ratio (SNR) evaluated from power spectra [7,15,21]. Other measures, such as bifurcation diagrams of peak amplitude and inter-spike intervals (ISI), normalized standard deviation (NSD) of peak amplitude (amplitude coherence) and NSD of ISI (time coherence), and Lyapunov exponents were also used [12,13]. In this paper we will apply different kinds of analysis to measure the network coherence, in particular, time series analysis, spectral analysis and correlation analysis. We will also study synchronization in order to know whether or not it is related to the coherence.

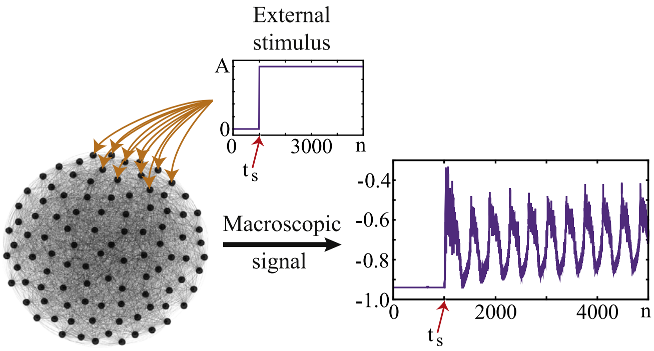

Fig. 1. Research design. The external stimulus with amplitude A is applied at time t_s to excite Na neurons in the network of N neurons. The macroscopic signal is the time series averaged over all neurons in the network.

2. The model

Each Rulkov neuron [16] in noisy environment is described by the following system of equations

$$\begin{aligned} x_{n+1} &= f(x_n, x_{n-1}, y_n + \beta_n), \\ y_{n+1} &= y_n - \mu(x_n + 1) + \mu\sigma + \mu\sigma_n + \mu A^{\xi}\xi_n, \end{aligned} \tag{1}$$

where x and y are fast and slow variables associated with membrane potential and gating variables, respectively, α, σ and $\mu \in (0, 1]$ are parameters which regulate the system dynamics, ξ is Gaussian noise with zero mean and unity standard deviation, A^{ξ} is the noise amplitude, and f is a piecewise function defined as

$$f(x_n, x_{n-1}, y_n) = \begin{cases} \alpha/(1 - x_n) + y_n, & \text{if } x_n \le 0, \\ \alpha + y_n, & \text{if } 0 < x_n < \alpha + y_n \text{ and } x_{n-1} \le 0, \\ -1, & \text{if } x_n \ge \alpha + y_n \text{ or } x_{n-1} > 0, \end{cases} \tag{2}$$

constructed in a way to reproduce different regimes of neuron-like activity, such as spiking, bursting and silent regimes. Here, β_n and σ_n are parameters related to external stimuli and defined as

$$\begin{aligned} \beta_n &= \beta^e I_n^{ext} + \beta^{syn} I_n^{syn}, \\ \sigma_n &= \sigma^e I_n^{ext} + \sigma^{syn} I_n^{syn}, \end{aligned} \tag{3}$$

where β^e and σ^e are coefficients used to balance the effect of external current I_n^{ext} defined as

$$I_n^{exp} = \begin{cases} 0, & n < t_s, \\ A, & n \ge t_s, \end{cases} \tag{4}$$

β^{syn} and σ^{syn} are coefficients of chemical synaptic coupling [20], and I_n^{syn} is a synaptic current given as

$$I_{n+1}^{syn} = \gamma I_n^{syn} - g_{syn} * \begin{cases} (x_n^{post} - x_{rp})/(1 + e^{-k(x_n^{post} - \theta)}), & \text{when } x_n^{pre} \ge \alpha + y_n^{pre} + \beta_n^{pre}, \\ 0, & \text{otherwise}, \end{cases} \tag{5}$$

where $g_{syn} \ge 0$ is the strength of synaptic coupling, $\theta = -1.55$ and $k = 50$ are synaptic parameters which stand for the synaptic threshold behavior. The super indices *pre* and *post* refer, respectively, to the presynaptic and postsynaptic variables, $\gamma \in [0, 1]$ is the synaptic relaxation time defining a portion of synaptic current preserved in the next iteration, and x_{rp} is a reversal potential determining the type of synapse, inhibitory or excitatory. The parameter values are chosen so that uncoupled neurons are in a resting state, namely, $\alpha = 3.65$, $\sigma = 0.06$ and $\mu = 0.0005$. We also assume $\beta^e = 0.133$, $\sigma^e = 1.0$, $\beta^{syn} = 0.1$, $\sigma^{syn} = 0.5$ and $x_{rp} = 0$.

The research design is shown in Fig. 1. We consider a network of N globally coupled neurons with random coupling strength $g_{syn} \in [0, 1]$ and relaxation time $\gamma \in [0, 0.5]$.

Without external stimulation and in the absence of noise, all neurons are in a silence regime. The external current in the form of a rectangular pulse with amplitude A is applied to Na neurons at time t_s. This stimulation excites Na neurons, which in turn excite other neurons in the network. Since the coupling strength is random, some of the neurons fire in a periodic spiking regime, some in an irregular bursting regime, and some remain in a silent state. Here, we are interested in macroscopic dynamics representing the global network behavior. The macroscopic signal shown in the right-hand panel of Fig. 1 exhibits the time series of the fast variable x averaged over all neurons in the network.

3. The analysis

In this section we will show how regularity of the macroscopic signal depends on the number of stimulated neurons Na, the network size N, the amplitude of external stimulus A, and the amplitude of noise A^{ξ}. We will start with the time series analysis, and

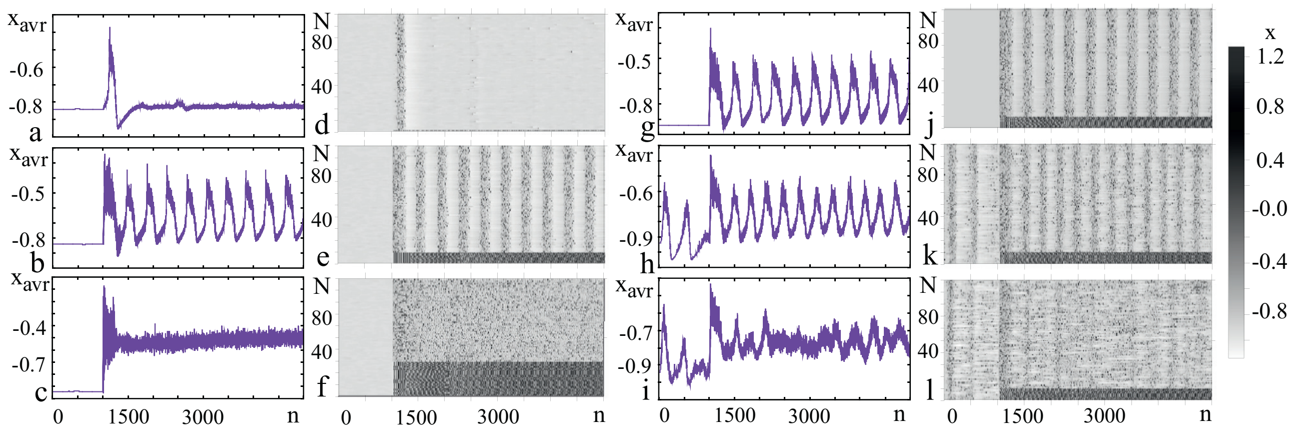

Fig. 2. (a-c,g-i) Time series of average membrane potential and (d–f,j–l) membrane potential of all neurons in the network of $N = 100$ neurons, when the stimulus with amplitude $A = 1$ is applied to (a,d) $Na = 1$ neuron, (b,e) $Na = 10$ neurons, and (c,f) $Na = 30$ neurons, under noise with amplitude $A^{\xi} = 0.1$, and when internal noise amplitude is (g,j) $A^{\xi} = 0$, (h,k) $A^{\xi} = 1$, and (i,l) $A^{\xi} = 2$ for the case of 10 stimulated neurons.

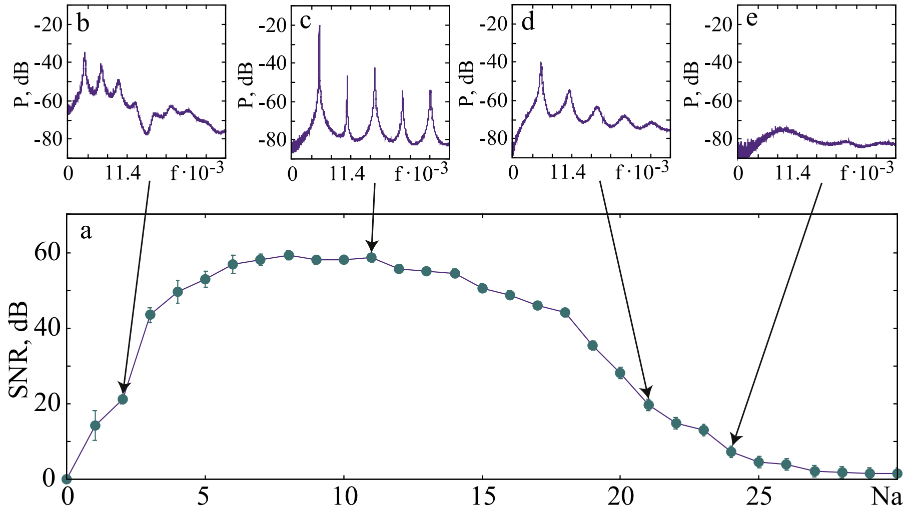

Fig. 3. (a) Signal-to-noise ratio (SNR) versus the number of stimulated neurons Na and (b–e) power spectra of average membrane potential for (b) $Na = 2$, (c) $Na = 11$, (d) $Na = 21$, and (e) $Na = 24$ for $A^{\xi} = 0.1$, $A = 1$, and $N = 100$.

proceed to analysis of the power spectrum and self-correlation. Finally, we will study synchronization.

3.1. Time series analysis

In the Fig. 2 (a–c) we show the time series of the average membrane potential

$$x_{avr} = \frac{1}{N}\sum_{i=1}^{N} x_i \tag{6}$$

where i is an index of neuron, $N = 100$ is the number of neurons in the network. In the 2 (d–f) panels we plot the time series of the membrane potentials of all neurons in the network. One can see that the vertical dark lines for $Na = 10$ (e) form a periodic structure, thus indicating regularity in the inter-spike intervals (ISI) in contradistinction to cases of $Na = 1$ and $Na = 30$ when there is only one group of spikes can be observed in the beginning of external stimulus appliance (d) or there are no grouping at all due to neurons irregularly spiking. Similar results were obtained for the network of 50 neurons.

The effect of noise is illustrated in Fig. 2 (g–l). One can see that increasing noise amplitude leads to decreasing regularity. Averaged signal starts to be more noise, each neuron herewith starts spiking chaoticly. But one still can see groups in the signal but they are irregular now. We should note that this is true only for this set of parameters. As distinct from the previous case, the macroscopic signals shown Fig. 2 (h,i,k,l) represent spiking dynamics before the stimulus is applied, i.e. for $n < 1000$. The spiking behavior without external stimulation is induced by the relatively strong noise.

3.2. Power spectrum analysis

Next, we will study coherence using the signal-to-noise ratio (SNR) derived from the power spectrum. In the upper panels of Fig. 3 we show the power spectra of the average membrane potential x_{avr} of all neurons in the network. The maximum power in the spectrum $P_{\max}$ appears at the average frequency of spiking neurons f_s. Therefore, this spectral component reflects the contribution of a regular behavior, while the noise contributes mainly to the background component P_N at the same frequency f_s [7,21,22]. The signal-to-noise ratio can be calculated from the power spectra as $\text{SNR} = P_{\max} - P_N$ (dB) at the dominant frequency f_s.

The dependence of SNR on the number of stimulated neurons is shown in the lower panel of Fig. 3. One can see that with increasing Na, SNR first increases rapidly for small values of Na reaching the maximum value for $Na \in [6,\ 11]$, and then gradually decreases to 0. This means that the network coherence has a reso-

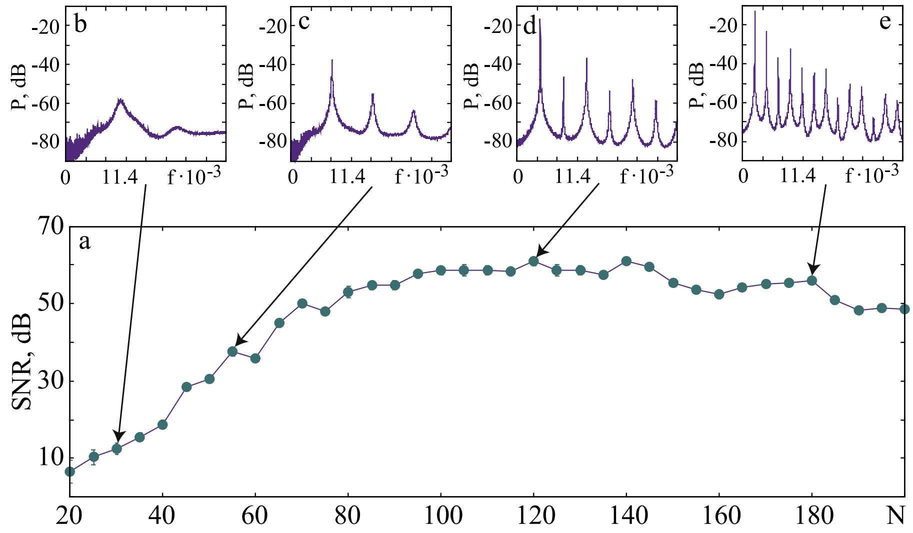

Fig. 4. (a) Signal-noise ratio (SNR) versus network size N for $A^{\xi} = 0.1$, $A = 1$, $Na = 10$ and (b–e) power spectra for (b) $N = 30$, (c) $N = 55$, (d) $N = 120$, and (e) $N = 180$.

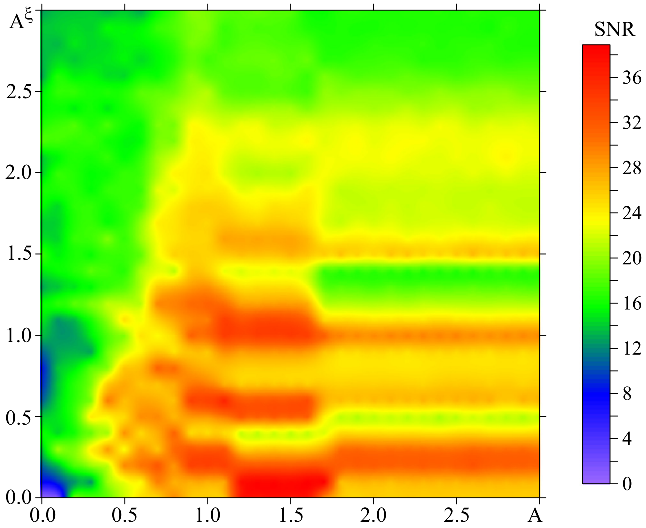

Fig. 5. Signal-to-noise ratio (SNR) in the parameter space of stimulus A and noise A^{ξ} amplitudes. The SNR value is represented by the color scheme shown in the right panel.

nant character with respect to the number of stimulated neurons. We can also note that increasing the number of stimulated neurons leads to slowly increasing the main frequency. As one can see from power spectra for $Na = 2$ and $Na = 21$, when SNR= 20 noise background is high and maximum power is not so big. But for the resonance maximum we have a high peak at the main frequency and low noise. And for big values of number of stimulated neurons both $P_{\max}$ and P_N are very small.

In Fig. 4, where we plot the dependence of the SNR on the number of neurons in the network one can see as N is increased, the SNR gradually increases too, reaching the maximum for the network size near 120, and then the SNR almost doesn't change for larger networks. Simultaneously, the dominant frequency decreases (ISI increases), as one can see from the power spectra in the upper panels. At the same time, the maximum power at the main frequency are also increasing while background noise remains the same. Also we can note that increasing network size leads to increasing number of harmonics and subharmonics in power spectra.

In Fig. 5 we show the dependence of SNR on the stimulus A and noise A^{ξ} amplitudes, on which one can see the existence of various coherence resonances (dark regions) in the parameter space. If we fix value of A^{ξ} in the range from 0 to 2.3 and increase A from 0 to 3, we observe a resonant phenomenon when SNR is increasing at the beginning, reaching the maximum, then decreasing for some value and staying the same in the end. Also we should note that this phenomenon of SNR being the same for $A > 1.75$ is true for all observed values of noise. On the other hand, increasing noise amplitude when stimulus amplitude is fixed, can give the alternation of maxima and minima for $A > 0.5$. We should note that for $A^{\xi} > 2.3$ and $A < 0.5$ there is no resonance. Thus, in the range $0.8 < A < 1.75$ we observe three main areas of coherent resonance: $0 < A^{\xi} < 0.3$, $0.45 < A^{\xi} < 0.7$, and $0.9 < A^{\xi} < 1.2$.

3.3. Correlation analysis

Following the approach proposed by Pikovsky and Kurths [6], we characterized the coherence by the correlation time defined as

$$\tau_c = \sum_{n_0}^{T} C(\tau)^2, \qquad (7)$$

where n_0 is the number of iterations corresponding to transients, T is the total number of iterations in time series, $C(\tau)$ is the autocorrelation function given as

$$C(\tau) = \frac{\left\langle (x_{avr}(n) - \langle x_{avr} \rangle)(x_{avr}(n+\tau) - \langle x_{arv} \rangle) \right\rangle}{\left\langle (x_{avr}(n) - \langle x_{avr} \rangle)^2 \right\rangle}, \qquad (8)$$

where $\langle \ldots \rangle$ is the time average after transients. The larger the correlation time, the better the coherence.

In Figs. 6 we plot the dependence of natural logarithm of correlation time on the number of stimulated neurons Na, network size N, stimulus amplitude A and noise amplitude A^{ξ}. The areas with higher coherence are clearly distinguished in the diagrams. On Fig. 6 (a) one can the same dependencies from Na and N as on Figs. 3 and 4. From Fig. 6 (a) we can definitely say that there is resonance with respect to the number of stimulated neurons and to the network size. On the Fig. 6 (b) one can see complex dependence on which small white curves of maximum values of characteristic correlation time are exist in the are of $0.5 < A < 1.25$ and $0.2 < A^{\xi} < 1.0$. This area of parameters value is similar to the one from Fig. 5 observed before.

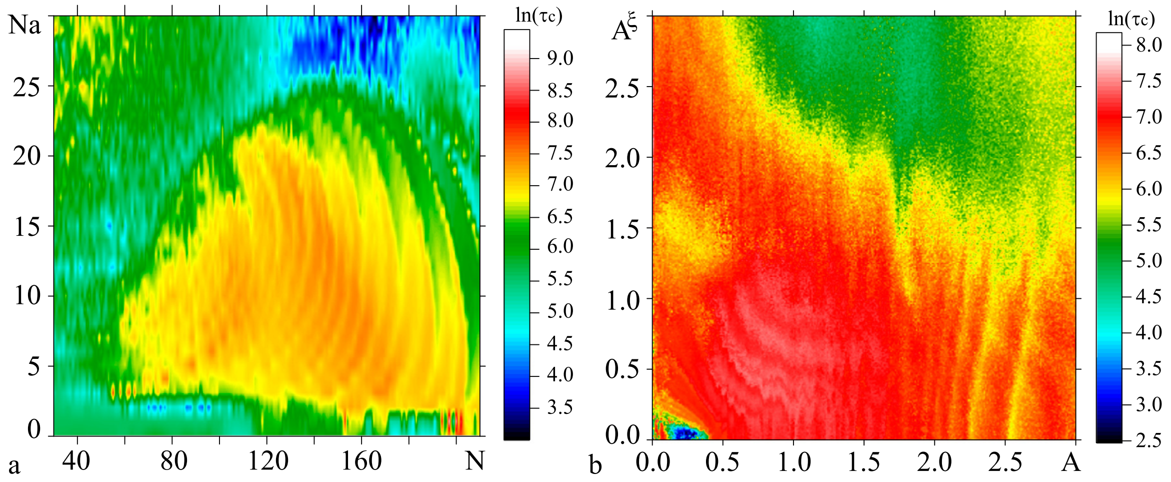

Fig. 6. Two-parameter diagram of natural logarithm of characteristic correlation time in the space of (a) network size N and number of stimulated neurons Na for $A^{\xi} = 0.1$ and $A = 1$ and (b) stimulus A and noise A^{ξ} amplitudes for $N = 100$ and $Na = 10$.

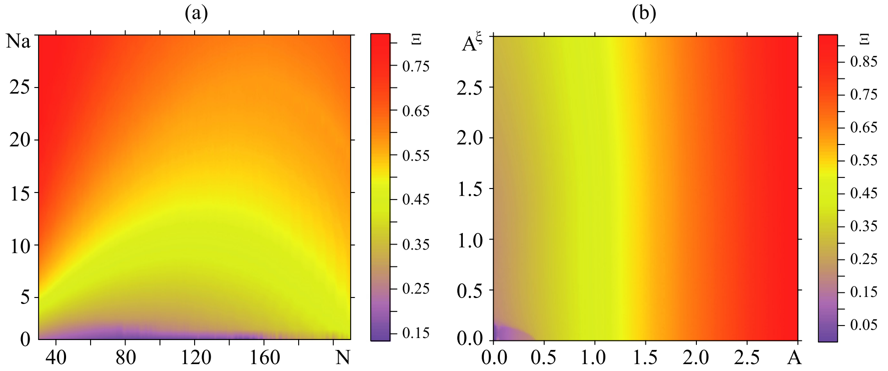

Fig. 7. Synchronization index in two-parameter space of (a) network size and the number of stimulated neurons for $A = 1$ and $A^{\xi} = 0.1$ and (b) stimulus and noise amplitudes for $N = 100$ and $Na = 10$.

3.4. *Synchronization*

The above analysis of the network coherence can raise the question: Is the improving coherence associated with enhancing synchronization? To answer this interesting question we calculate the network synchronization index as follows [23,24]

$$\Xi = \sqrt{\frac{1}{T - n_0} \sum_{n=n_0+1}^{T} \xi_n}, \tag{9}$$

where ξ_n is the standard deviation given as

$$\xi_n = \frac{1}{N} \sum_{i=1}^{N} \left(x_n^{(i)}\right)^2 - \left(\frac{1}{N} \sum_{i=1}^{N} x_n^{(i)}\right)^2. \tag{10}$$

The smaller Ξ, the better the synchronization; $\Xi = 0$ means complete synchronization.

The dependence of the synchronization index on the control parameters is shown in Fig. 7.

The comparison of the synchronization diagrams with the coherence diagrams does not reveal notable correlation. The extremum in the synchronization index is only observed with respect to the network size. Indeed, as one can see from Figs. 7(a), synchronization is enhanced for $N = 120$ that coincides with the maximum in the SNR in Fig. 4. However, no resonances are detected with respect to other control parameters. Such incoincidence can be explained by the fact that the synchronization index given by Eq. (9) is valid only for the estimation of synchronization in systems with a single time scale. Although the neuronal network can have two time scales corresponding to spiking and bursting dynamics. In our network, the neurons can be synchronized by bursts, but not by spikes. Furthermore, the neurons with irregular (chaotic) dynamics can be well synchronized, while the network coherence is very low due to irregular oscillations. Therefore, better synchronization means better coherence only if all neurons in the network are in a regular spiking regime.

4. Conclusion

We have shown that regularity in the collective spiking behaviour of a neuronal network maximizes at a certain level of intrinsic noise, external stimulus, network size, and the number of stimulated neurons. This coherence resonance phenomenon has been found in the signal-to-noise ratio, calculated from the average power spectra of the neuronal network, and in the correlation time.

By studying network synchronization we found that overall synchronization of the neurons became worse as noise, or amplitude of external stimulus, or the number of stimulated neurons is increased. A non-monotonic dependence of synchronization has only been observed with respect to the network size. The difference between uncorrelated behavior in the coherence and synchronization can be explained by the existence of two different time scales in neural dynamics, spiking and bursting. Being synchronous by bursts, the neurons can be asynchronous by spikes. Therefore, overall synchronization does not reflect the network coherence.

We believe that our results will stimulate further research in this direction. Since the signal-to-noise ratio can be improved by adjusting the network size, intrinsic noise, and the number of stimulated neurons, the answer to the question: Does the brain work in coherence resonance to detect a weak stimulus? can be positive. In order to check this hypothesis, specific neurophysiological experiments are required. These experiments can be designed using the approach proposed in our paper, for example, by studying a macroscopic signal in a neural culture grown in a multi-electrode matrix or by estimating brain noise from electro- or magneto-encephalographic data [4].

Acknowledgments

This work has been supported by the Russian Science Foundation (grant 17-72-30003) in the part of numerical simulation and analysis. A. N. P. acknowledges support from the Ministry of Economy and Competitiveness (Spain) (project SAF2016-80240) for the model development.

References

[1] Deco G. Stochastic dynamics as a principle of brain function. Prog Neurobiol 2009;88:1–16.

[2] Kelso JAS. Dynamic patterns: The self-organization of brain and behavior. Cambridge Bradford Books; 1997.

[3] Pisarchik AN, Jaimes-Retegui R, Magall-Garca CDA, Castillo-Morales CO. Critical slowing down and noise-induced intermittency in bistable perception. Biol Cybern 2014;108:397–404.

[4] Runnova AE, Hramov AE, Grubov VV, Koronovskii AA, Kurovskaya MK, Pisarchik AN. Theoretical background and experimental measurements of human brain noise intensity in perception of ambiguous images. Chaos Solitons Fractals 2016;93:201–6.

[5] Simonotto E, Riani M, Seife C, Roberts M, Twitty J, Moss F. Visual perception in stochastic resonance. Phys Rev Lett 1997;78:1186–9.

[6] Pikovsky AS, Kurths J. Coherence resonance in a noise-driven excitable system. Phys Rev Lett 1997;78:775–8.

[7] Neiman A, Saparin PI, Stone L. Coherence resonance at noisy precursors of bifurcations in nonlinear dynamical systems. Phys Rev E 1997;56:270–3.

[8] Pikovsky A, Zaikin A, de laCasa MA. System size resonance in coupled noisy systems and in the Ising model. Phys Rev Lett 2002;88. 050601.

[9] Yilmaz E, Ozer M, Baysal V, Perc M. Autapse-induced multiple coherence resonance in single neurons and neuronal networks. Sci Rep 2016;6. 30914.

[10] Toral R, Mirasso CR, Gunton JD. System size coherence resonance in coupled Fitzhugh–Nagumo models. Europhys Lett 2003;61:162–7.

[11] Martinez Avila JF, Cavalcante HLD, de S, Rios Leite JR. Experimental deterministic coherence resonance. Phys Rev Lett 2004;93. 144101.

[12] Pisarchik AN, Jaimes-Reátegui R. Deterministic coherence resonance in coupled chaotic oscillators with frequency mismatch. Phys Rev E 2015;92. 050901(R).

[13] García-Vellisca MA, Pisarchik AN, Jaimes-Reátegui R. Experimental evidence of deterministic coherence resonance in coupled chaotic systems with frequency mismatch. Phys Rev E 2016;94. 012218.

[14] Gammaitoni L, Hänggi P, Jung P, Marchesoni F. Stochastic resonance. Rev Mod Phys 1998;70:223–87.

[15] Pisarchik AN, Corbalán R. Stochastic resonance in a chaotic laser. Phys Rev E 1998;58:R2697–700.

[16] Rulkov NF, Timofeev I, Bazhenov M. Oscillations in large-scale cortical networks: map-based model. J Comput Neurosci 2004;17:203–23.

[17] Ferrari FAS, Viana RL, Gomez F, Lorimer T, Stoop R. Macroscopic bursting in physiological networks: node or network property? New J Phys 2015;17:055024.

[18] Lehnertz K, Elger CE. Can epileptic seizures be predicted? evidence from nonlinear time series analysis of brain electrical activity. Phys Rev Lett 1998;80:5019–22.

[19] Angelini L. Steady-state visual evoked potentials and phase synchronization in migraine patients. Phys Rev Lett 2004;93. 038103.

[20] Hu D, Cao H. 2016 Stability and synchronization of coupled Rulkov map-based neurons with chemical synapses. Commun Nonlinear Sci Numer Simulat 2016;35:105–22.

[21] Campos-Mejía A., Pisarchik A.N., Arroyo-Almanza D.A.. Noise-induced onoff intermittency in mutually coupled semiconductor lasers. Chaos Solitons Fractals; 54:96–100.

[22] Huerta-Cuellar G, Pisarchik AN, Kiryanov AV, Barmenkov YO, del Valle HJ. Prebifurcation noise amplification in a fiber laser. Phys Rev E 2009;79. 036204.

[23] Wang Q, Perc M, Duan Z, Chen G. Synchronization transitions on scale-free neuronal networks due to finite information transmission delays. Phys Rev E 2009;80. 026206.

[24] Sausedo-Solorio JM, Pisarchik AN. Synchronization in network motifs of delay–coupled map-based neurons. Eur Phys J Spec Topics 2017;226:1911–20.